Impact of N-induced potential fluctuations on the electron transport in Ga(As,N)

F. Ishikawa,[a] G. Mussler, K.-J. Friedland, H. Kostial, K. Hagenstein, L. Däweritz, and K. H. Ploog
Paul-Drude-Institut für Festkörperelektronik, Hausvogteiplatz 5–7, 10117 Berlin, Germany

(Received 29 August 2005; accepted 3 November 2005; published online 27 December 2005)

We investigate the electron transport in Ga(As,N) layers focusing on the influence of potential fluctuations. With increasing electron concentration, a metal-insulator transition is observed in the temperature dependence of the resistivity for a series of samples containing 0.8% of N. The observed behavior is discussed in the frame of Anderson transition. By increasing the N concentration up to 2.2%, we observe an increase of the potential fluctuations' amplitude. Mean-square values for the intrinsic N-induced fluctuation γ_N are obtained from percolation theory to be larger than 30 meV. Rapid thermal annealing reduces γ_N significantly for samples with higher N concentration. These large potential fluctuations lead to electron localization and induce thermally activated conductivity which is observable up to 300 K. © *2005 American Institute of Physics*. [DOI: 10.1063/1.2158511]

Dilute nitride alloys based on Ga(As,N) are materials of great physical and technological importance due to the tunability of their band gap. The incorporation of a few percent of nitrogen into the GaAs host splits the conduction band (CB) into two bands and thus leads to an anomalous reduction of the band gap.[1,2] Furthermore, a drastic increase of the electron effective mass is observed.[3] These specific features have been successfully explained by several models,[2,3] particularly the band anti-crossing (BAC) model which considers the interaction between a localized N-related state and the extended CB states of the host material.[2] Despite these interesting properties, the incorporation of N deteriorates the electrical and optical properties of the material by a formation of growth-induced defects.[4] Nevertheless, these properties can be efficiently improved by postgrowth annealing, such as rapid thermal annealing (RTA).[4–6] On the other hand, the inevitable structural inhomogeneity of alloys[7] and the large differences in electronegativity between the binary constituents cause intrinsic potential fluctuations.[6,8] The existence of potential fluctuations and the resulting carrier localization[9] will affect carrier transport and device performance.[6,10] This letter reports on the transport characteristics of *n*-type Ga(As,N) layers focusing on the role of potential fluctuations and their dependence on postgrowth RTA.

All the samples were grown on semi-insulating GaAs (001) substrates using a solid-source molecular-beam epitaxy system. Nitrogen was supplied by an rf plasma source. Si was used for *n*-type doping. Prior to the growth of Ga(As,N), a 400-nm-thick undoped GaAs buffer layer was grown at 580 °C. Subsequently, Si doped Ga(As,N) films were grown at 450 °C with N contents of 0.8%, 1.7%, and 2.2%. The N concentration was varied by changing the N_2-flow rate and plasma power. For the sample with 0.8% N, the electron concentration was also varied by changing the Si concentration. Table I summarizes the parameters of the samples under investigation. The thickness of the Ga(As,N) layers ranges between 500 and 700 nm. These layer thicknesses were chosen such that both strain relaxation and carrier depletion from surface/interface states throughout the layer were prevented. The N content in Table I was obtained by fitting ω-2θ x-ray diffraction scans with a simulation based on the dynamical diffraction theory. The electron concentration n and the mobility μ were obtained from Hall effect measurements on samples in the van der Pauw geometry at 300 K. The density of silicon (N_{Si}) is assumed to be equal to the electron concentration in GaAs layers grown under identical conditions, where $n \cong N_{Si}$ at $n \leqslant 5 \times 10^{18}$ cm^{-3}.[11] Postgrowth RTA was carried out to remove growth-induced defects.[4,5] The samples were heated to 800 °C for 60 s in a N_2 ambient.[5] After RTA, all the samples showed 4–15 times higher photoluminescence intensities; μ clearly increased for all the samples, and n also increased for all the samples except one. These data confirm that RTA generally improves the mobility and the activation of the donors by the removal of defects, resulting in an improvement of the electrical and optical properties.[4–6] The observed n and μ are also summarized in Table I. To study the electron transport in these samples in more detail, we carried out temperature-dependent resistivity and Hall effect measurements in the van der Pauw geometry in the temperature range from 77 to 300 K.

Figure 1 shows the temperature dependence of the resistivity for a series of samples containing 0.8% of N with different n. The results show a behavior similar to a metal-insulator transition. The samples with lower n (081, 081a) exhibit insulator-like conductivity, while the conduction of samples with higher n appears metallic-like. This behavior can be understood in the frame of Anderson transition, in which potential fluctuations in the CB are represented by periodically arranged potential wells with random depth.[12,13] Consequently, localized states are created which are separated from the delocalized states by a boundary. By varying the number of electrons in the CB, the Fermi level will shift with respect to the band, and it may cross the boundary between the localized and delocalized states. As a result, a metal-insulator transition is observed. The characteristics of

[a]Author to whom correspondence should be addressed; electronic mail: ishikawa@pdi-berlin.de

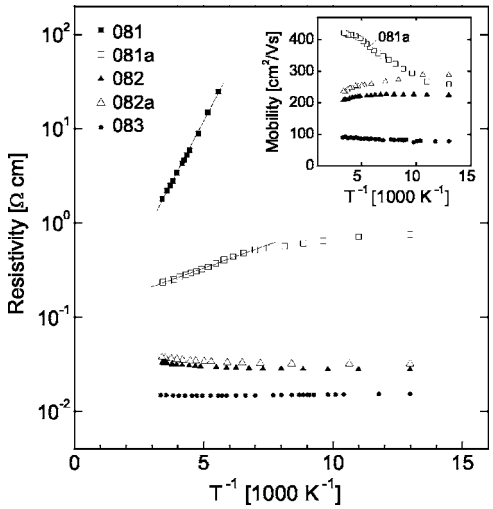

FIG. 1. Temperature dependence of the resistivity for samples containing 0.8% N with different electron concentrations. The inset shows the mobility for the corresponding samples. The solid lines are least-square linear fits of the data.

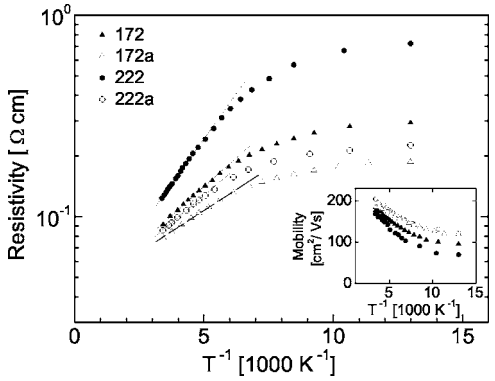

FIG. 2. Temperature dependence of the resistivity for samples containing 1.7% and 2.2% N. The inset shows the mobility for the corresponding samples. The solid lines are least-square linear fits of the data.

the temperature-dependent mobilities also imply the presence of carrier localization.[14] For the metallic-like samples 082 and 082a, μ decreases with increasing temperatures near room temperature, which is the commonly observed behavior for III-V semiconductors. In contrast, the insulator-like sample 081a shows an increasing μ with temperature as seen in the inset of Fig. 1, which is an indication of an increasing participation of delocalized states in the transport.

In the following, we discuss the localization of carriers quantitatively by considering the activation energy and the chemical potential. When the electrons occupy localized states, the transport is possible by thermal activation into delocalized states.[12,13] This leads to an exponential temperature dependence of the resistivity ρ with a specific activation energy E_a which is usually determined at high temperatures,[12,13] given by $\rho=\rho_0 \exp(E_a/k_BT)$. Here, ρ_0 is a constant, k_B refers to the Boltzmann constant, and T is the temperature. The fits of the data with this equation are shown by solid lines in Fig. 1 and return values for the activation energy as listed in Table I. The electrons have a chemical potential ξ which depends on n. The value of ξ was calculated using the value obtained from Hall effect measurements at 300 K by $\xi=\hbar^2\cdot(3\pi^2 n)^{2/3}/2m$. Here, m is the electron effective mass depending on the N content of Ga(As,N), for which we use the values from the BAC theory.[3] The calculated ξ values for our samples are summarized in Table I. E_a reflects the energy from the Fermi energy ξ to the energy above of which metallic transport occurs, i.e., the percolation threshold V_p.[12,13] Hence, we estimate the magnitude of the potential fluctuation V_p as

$$V_p = \xi + E_a. \tag{1}$$

The obtained values of V_p are depicted in Table I. A metallic-like conductivity will be obtained above the percolation threshold when $\xi > V_p$ with vanishing E_a. This case is indicated as *metallic* in Table I. Sample 081 exhibits a very large E_a and a high resistivity which increases exponentially with $1/T$. This feature is probably due to the negligible contribution of delocalized states to the carrier transport.[13] Therefore, for sample 081, we assumed that the determination of μ and ξ, and the discussion using Eq. (1), is in principle not possible.

Figure 2 shows the temperature dependence of the resistivity of the as-grown and annealed samples with 1.7% and 2.2% N (samples 172, 172a, 222 and 222a). Thermally activated conductivities were observed for these samples, similar to the samples 081/081a in Fig. 1. The mobility of all the samples showed a clear increase for higher temperatures as before.[14] The values for E_a and V_p from these samples are also summarized in Table I. Hence, by increasing the N concentration up to 2.2%, a clear increase of V_p compared to the sample with 0.8% N can be observed. V_p is reduced upon annealing, and this effect is more pronounced for the sample with higher 2.2% N content.

TABLE I. Properties of the investigated Ga(As,N) samples. Listed are the sample numbers ("a" indicates the annealed samples), the N concentration, the nominal Si concentration N_{Si}, and electron concentration n and Hall mobility μ at 300 K. also shown are the calculated chemical potential ξ from n at 300 K, the activation energy E_a obtained by the linear fits shown in Figs. 1 and 2, and the energy position of the percolation threshold V_p.

Sample	N(%)	N_{Si}(cm^{-3})	n(cm^{-3})	μ(cm^2/V s)	ξ(meV)	E_a(meV)	V_p(meV)
081	0.8	1.0×10^{17}	3.4×10^{16}	⋯	⋯	104	⋯
081a			9.4×10^{16}	413	8	19	27
082	0.8	1.0×10^{18}	1.0×10^{18}	208	40	⋯	Metallic
082a			8.2×10^{17}	240	34	⋯	Metallic
083	0.8	1.0×10^{19}	5.1×10^{18}	89	115	⋯	Metallic
172	1.7	1.0×10^{18}	4.9×10^{17}	176	22	23	45
172a			5.3×10^{17}	185	23	16	39
222	2.2	1.0×10^{18}	3.9×10^{17}	168	18	35	53
222a			4.6×10^{17}	201	21	22	43

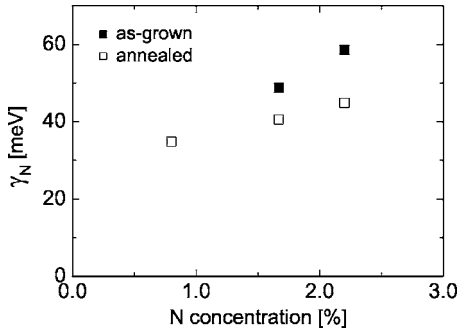

FIG. 3. Mean square N induced potential fluctuation γ_N as a function of the N concentration.

Finally, we discuss the potential fluctuation in the framework of percolation theory with two conceivable assumptions. First, we assume that the potential fluctuations are randomly distributed. In this case, the mean-square values of the potential fluctuation γ_{meas} become $V_p = 0.67\ \gamma_{meas}$.[12] Second, we assume that γ_{meas} consists of two parts,[12,15] the intrinsic N-induced fluctuation γ_N and an additional fluctuation γ_D:

$$\gamma_{meas} = \gamma_N + \gamma_D. \tag{2}$$

The doping induced potential fluctuation γ_D is obtained by the Coulomb interaction of the impurities,[12,15,16] which can be expressed with the electron charge e and the vacuum permittivity ε_0 by

$$\gamma_D = \frac{e^2}{4\pi\varepsilon_0\varepsilon} \cdot \frac{N_t^{2/3}}{n^{1/3}} = \frac{e^2}{4\pi\varepsilon_0\varepsilon} \cdot \frac{\{(1+K)N_{Si}\}^{2/3}}{n^{1/3}}. \tag{3}$$

N_t is the total concentration of donors and compensating acceptors. K is the degree of compensation obtained by $K = (N_{Si} - n)/N_{Si}$; ε is the static dielectric constant and we assume that it bears the same value $\varepsilon = 12.9$ as for GaAs independent of the N content.[17] The obtained γ_N is plotted in Fig. 3. We find γ_N to be larger than 30 meV, and its value increases with increasing N concentration. The RTA treatment reduces γ_N significantly for samples with higher N concentration.

In conclusion, we have investigated the transport characteristics of Ga(As,N) focusing on the influence of potential fluctuations. We observe a metal-insulator transition which can be described in the frame of Anderson transition. We calculated the N-induced potential fluctuation γ_N, which increases with increasing N concentration. The RTA treatment reduces γ_N significantly for samples with higher N concentration. The large potential fluctuations can explain the thermally activated conductivity which can be observed up to 300 K.

One of the authors (F.I.) thanks O. Brandt and D. Kolovos-Vellianitis for critical reading of the manuscript.

[1] M. Weyers, M. Sato, and H. Ando, Jpn. J. Appl. Phys., Part 2 **31**, L853 (1992).
[2] W. Shan, W. Walukiewicz, J. W. A. III, E. E. Haller, J. F. Geisz, D. J. Friedman, J. M. Olson, and S. R. Kurz, Phys. Rev. Lett. **82**, 1221 (1999).
[3] C. Skierbiszewski, I. Gorczyca, S. P. Łepkowski, J. Łusakowski, J. Borysiuk, and J. Toivonen, Semicond. Sci. Technol. **19**, 1189 (2004).
[4] S. G. Spruytte, C. W. Coldren, J. S. Harris, W. Wampler, P. Krispin, K. H. Ploog, and M. C. Larson, J. Appl. Phys. **89**, 4401 (2001).
[5] G. Mussler, J.-M. Chauveau, A. Trampert, M. Ramsteiner, L. Dweritz, and K. H. Ploog, J. Cryst. Growth **267**, 60 (2004).
[6] S. R. Kurtz, N. A. Modine, E. D. Jones, A. A. Allerman, and J. F. Klem, Semicond. Sci. Technol. **17**, 843 (2002).
[7] I. Ho and G. B. Stringfellow, J. Cryst. Growth **178**, 1 (1997).
[8] J. W. Harrison and J. R. Hauser, Phys. Rev. B **13**, 5347 (1976).
[9] I. Buyanova, W. Chen, and B. Monemar, MRS Internet J. Nitride Semicond. Res. Semicond. Res. **6**, 2 (2001).
[10] R. J. Welty, H. Xin, C. W. Tu, and P. M. Asbeck, J. Appl. Phys. **95**, 327 (2004).
[11] Y. G. Chai, R. Chow, and C. E. C. Wood, Appl. Phys. Lett. **39**, 800 (1981).
[12] B. I. Shklovskii and A. L. Efros, *Electronic Properties of Doped Semiconductors* (Springer, Berlin, 1984), Chap. 13, p. 295.
[13] O. Madelung, *Introduction to Solid State Theory* (Springer, Berlin, 1978), Chap. 10, p. 435.
[14] J. Teubert, P. J. Klar, W. Heimbrot, K. Voltz, W. Stolz, P. Thomas, G. Leibiger, and V. Gottschalch, Appl. Phys. Lett. **84**, 747 (2004).
[15] H. Overhof and W. Beyer, Philos. Mag. B **47**, 433 (1983);
[16] J. A. Howard and R. A.Street, Phys. Rev. B **44**, 7935 (1991).
[17] G. Leibiger, V. Gottschalch, B. Rheinländer, J. Šilk, and M. Schubert, J. Appl. Phys. **89**, 4927 (2001).